

Journal of Astronomical Telescopes, Instruments, and Systems

AstronomicalTelescopes.SPIEDigitalLibrary.org

High-resolution, lightweight, and low-cost x-ray optics for the Lynx observatory

William W. Zhang
Kim D. Allgood
Michael P. Biskach
Kai-Wing Chan
Michal Hlinka
John D. Kearney
James R. Mazarella
Ryan S. McClelland
Ai Numata
Raul E. Riveros
Timo T. Saha
Peter M. Solly

William W. Zhang, Kim D. Allgood, Michael P. Biskach, Kai-Wing Chan, Michal Hlinka, John D. Kearney, James R. Mazarella, Ryan S. McClelland, Ai Numata, Raul E. Riveros, Timo T. Saha, Peter M. Solly, "High-resolution, lightweight, and low-cost x-ray optics for the Lynx observatory," *J. Astron. Telesc. Instrum. Syst.* **5**(2), 021012 (2019), doi: 10.1117/1.JATIS.5.2.021012.

SPIE.

High-resolution, lightweight, and low-cost x-ray optics for the Lynx observatory

William W. Zhang,^{a,*} Kim D. Allgood,^b Michael P. Biskach,^b Kai-Wing Chan,^c Michal Hlinka,^b John D. Kearney,^b James R. Mazzarella,^b Ryan S. McClelland,^a Ai Numata,^b Raul E. Riveros,^c Timo T. Saha,^a and Peter M. Solly^b

^aNASA Goddard Space Flight Center, Greenbelt, Maryland, United States

^bStinger Ghaffarian Technologies, Inc., Greenbelt, Maryland, United States

^cUniversity of Maryland-Baltimore County, Baltimore, Maryland, United States

Abstract. We describe an approach to build an x-ray mirror assembly that can meet Lynx’s requirements of high-angular resolution, large effective area, light weight, short production schedule, and low-production cost. Adopting a modular hierarchy, the assembly is composed of 37,492 mirror segments, each of which measures $\sim 100\text{ mm} \times 100\text{ mm} \times 0.5\text{ mm}$. These segments are integrated into 611 modules, which are individually tested and qualified to meet both science performance and spaceflight environment requirements before they in turn are integrated into 12 metashells. The 12 metashells are then integrated to form the mirror assembly. This approach combines the latest precision polishing technology and the monocrystalline silicon material to fabricate the thin and lightweight mirror segments. Because of the use of commercially available equipment and material and because of its highly modular and hierarchical building-up process, this approach is highly amenable to automation and mass production to maximize production throughput and to minimize production schedule and cost. As of fall 2018, the basic elements of this approach, including substrate fabrication, coating, alignment, and bonding, have been validated by the successful building and testing of single-pair mirror modules. In the next few years, the many steps of the approach will be refined and perfected by repeatedly building and testing mirror modules containing progressively more mirror segments to fully meet science performance, spaceflight environments, as well as programmatic requirements of the Lynx mission and other proposed missions, such as AXIS. © The Authors. Published by SPIE under a Creative Commons Attribution 4.0 Unported License. Distribution or reproduction of this work in whole or in part requires full attribution of the original publication, including its DOI. [DOI: [10.1117/1.JATIS.5.2.021012](https://doi.org/10.1117/1.JATIS.5.2.021012)]

Keywords: x-ray optics; silicon mirrors; lightweight optics.

Paper 18106SS received Nov. 5, 2018; accepted for publication Apr. 1, 2019; published online Apr. 26, 2019.

1 Introduction

The importance of x-ray optics to astronomy and astrophysics was recognized before extrasolar x-rays were discovered.¹ The half a century of x-ray astronomy is, to a great extent, a history of making ever better, lighter, and less expensive x-ray mirror assemblies for spaceflight, enabling ever more sensitive x-ray telescopes probing ever farther and earlier epochs of the Universe as well as ever fainter phenomena that occur in our own galaxy and in our own solar neighborhood. Two distinct categories of technologies have been used to make those mirror assemblies: direct fabrication and replication. These technologies each have their own advantages and disadvantages.

Direct fabrication is the traditional way of making high-quality optics for astronomy. It has been continually developed in the past four centuries. The fabrication process consists of grinding and polishing substrates with thickness of tens of millimeters, guided by precise measurement. It was naturally adopted as part of the first efforts in the 1960s to make x-ray optics. Those efforts focused on achieving the microroughness that is uniquely required and rather stringent for specularly reflecting x-rays in the band of 0.1 to 10 keV. Those efforts culminated in the Einstein Observatory² in the late 1970s, ROSAT³ in the early 1990s, and Chandra^{4,5} in the late 1990s. The x-ray mirror assemblies on these three observatories share the common characteristics of excellent angular resolution each for its own times,

small photon-collecting areas, and high-production costs. The small photon-collecting areas are caused by two reasons. The first is the fact that the grinding and polishing process could only make thick mirrors because polishing stress would break thin substrates and the material removal must be infinitesimally small compared to substrate thickness so that stress generated or relieved during the polishing process would not lead to unpredictable figure change. The second is that the amount of mass that can be lifted by rockets and launched into space is very limited, precluding very large and heavy x-ray mirror assemblies.

Replication comes in three different flavors: replication with epoxy, electroforming, and thermal glass slumping. The x-ray mirror assemblies on EXOSAT⁶ and Suzaku⁷ were made with epoxy replication. Perhaps more spaceflight mirror assemblies were made by electroforming nickel than any other process. Among them are the mirror assemblies on Beppo-SAX,⁸ XMM-Newton,^{9,10} Swift,¹¹ and eROSITA¹² and ART-XC¹³ onboard the soon-to-be-launched Spectrum-Roentgen-Gamma (SRG) satellite. The two x-ray mirror assemblies on NuSTAR^{14,15} were made by thermally slumping thin glass sheets. All of these mirror assemblies share the common characteristics of relatively poor to moderate angular resolution, relatively large photon-collecting area, and moderate to low production costs (Table 1).

From the perspective of overall design and implementation geometry, x-ray mirror assemblies take one of two forms for their basic mirror elements: full shells or segments. Full shell construction was implemented for Einstein, EXOSAT, ROSAT, Chandra, Beppo-SAX, XMM-Newton, Swift, eROSITA, and

*Address all correspondence to William W. Zhang, E-mail: William.W.Zhang@nasa.gov

Table 1 Comparison of key parameters of the mirror assemblies on Chandra, NuSTAR, and Lynx. Lynx's challenges lie in the fourfold requirements of angular resolution, mirror surface area, mass, and production cost. Note that the numbers in the mass column include only the mass of the mirror elements, not the mass of the mechanical structures necessary to support them. In general, the mass of the structures is proportional to the mass of the mirror element.

	Angular resolution (arc sec HPD)	Mirror surface area (m ²)	Mass (kg)	Production cost (\$ in real year)	Note
Chandra	0.5	19	1,018	~500M (1999)	One assembly
NuSTAR	58	92	50	~15M (2012)	Two identical assemblies
Lynx	0.5	380	500	~500M (~2030)	One assembly

ART-XC. Segmented mirror construction was implemented for Suzaku and NuSTAR. Full shells and segments each have their own advantages and disadvantages. Full shells utilize the natural axial symmetry of x-ray optics, minimizing the number of mirror elements that must be fabricated and integrated. Their major disadvantages are that they require proportionally large infrastructure to make large-diameter shells, making the process prohibitively expensive if technically feasible at all. In particular, large and thin shells, such as 1 m in diameter and less than 1 m in thickness, become difficult, or nearly impossible, to fabricate, handle, and integrate. On the other hand, the segmented approach has the disadvantage of having to fabricate and integrate a very large number of small mirror segments, sacrificing the natural axial symmetry of x-ray optics. It has the advantage, however, of making potentially arbitrarily large mirror assemblies without having to build up proportionally large infrastructure. Perhaps more importantly because of the relatively small mirror segments, the segmented approach can make very lightweight mirrors and can make use of commercially available equipment, materials, and modern mass production technologies to minimize production schedule and cost. All things considered, we have adopted the segmented approach to making a mirror assembly for Lynx and other future x-ray missions, such as the Advanced X-Ray Imaging Satellite (AXIS).¹⁶

Since 2011, we have been developing a technology¹⁷ that combines precision polishing, which has been successfully used for making Chandra and other high quality optics, with monocrystalline silicon to make thin, lightweight, and high-quality mirror segments. In this paper, we first describe the overall approach to building a mirror assembly required for Lynx, clearly separating engineering elements and technology elements of the approach. Then, we describe the development of the technology elements to meet Lynx requirements.¹⁸

2 Hierarchical Metashell Approach

Designing, building, testing, and qualifying an x-ray mirror assembly for spaceflight is a significant undertaking, requiring efforts of many people over many years, and costing many millions of dollars. The success of the undertaking, while depending on many factors, critically depends on overall design of the mirror assembly, production process, and maturity of technical elements. For Lynx and similar missions like AXIS, we have adopted a modular and hierarchical approach to building, testing, and otherwise qualifying a mirror assembly, as shown in Fig. 1.

It takes four independent major steps to build a Lynx mirror assembly. In practice, these four steps will overlap in time and share facilities and personnel. In the first step, shown in

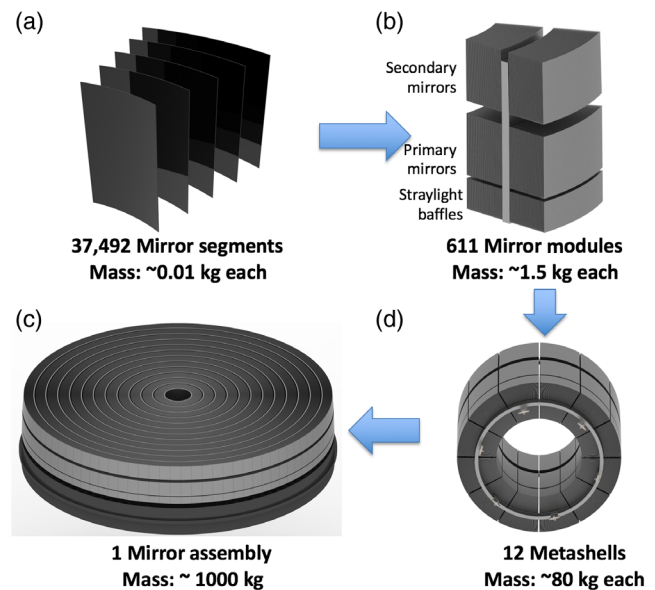


Fig. 1 The four major steps of building a mirror assembly for Lynx. (a) Fabrication and qualification of mirror segments, each measuring approximately 100 mm × 100 mm × 0.5 mm. (b) Those mirror segments are integrated into 611 mirror modules, each of which is independently built and tested. (c) The 611 mirror modules are in turn integrated into 12 metashells, each of which again is individually and independently built and tested. Finally, (d) The 12 metashells are integrated into a mirror assembly that will then be tested and otherwise qualified for spaceflight.

Fig. 1(a), 37,492 mirror segments are fabricated. Although they are of 914 different optical design prescriptions, 457 primary mirrors, and 457 secondary mirrors, they have similar dimensions, ~100 mm in the optical axis direction, 100 mm in the circumferential direction, and 0.5 mm in thickness. In the second step, shown in Fig. 1(b), these 37,492 mirror segments are integrated into 611 mirror modules, each of which, in addition to the mirror segments themselves, also includes a midplate, made of the same material as the mirror segments, onto which all the mirror segments are attached directly or indirectly via other mirror segments, and many nonreflecting stray light baffles. In the third step, shown in Fig. 1(d), the 611 mirror modules are integrated into 12 metashells, each of which contains 12 (innermost) to 91 (outermost) mirror modules. Finally, in the fourth step, the 12 metashells are integrated to make the assembly.

This hierarchical approach has many advantages. Each step is conceptually, technically, and programmatically isolated from

the others, therefore isolating and minimizing technical and programmatic risks. Each step has to fulfill its own obligations of delivering to the next step components that meet well-defined requirements, both in terms of science performance, such as angular resolution and effective area, and in terms of structural and environmental robustness. Another important advantage is that this approach separates and isolates the technology development effort, which must take place long before a mission is approved, from the engineering and programmatic effort, which can only take place after a mission is approved, that is necessary to successfully build a mirror assembly. This clear separation enables the most efficient use of technical and financial resources at different stages of the mission development.

Table 2 shows a top-level Lynx angular resolution error budget that is used to guide our technology development effort. In the following, we elaborate on each of the major steps that are necessary to build a Lynx mirror assembly.

2.1 Mirror Segments

Mirror segments are the basic elements needed to build a mirror assembly. Once top-level parameters of a telescope, such as focal length, mass, and effective area, are decided based on science requirements, the total mirror surface area and areal density, i.e., mass per unit mirror surface area, are determined as well. Furthermore, once a material is selected, its density

Table 2 Top-level angular resolution error budget guiding technology development to meet Lynx requirements. The hierarchical metashell approach isolates the technology development to the bold italic fonts, i.e., fabrication of mirror segments, and alignment and bonding of them to make mirror modules. All other items, such as integration of modules into metashells and, in turn, integration of metashells into assembly are challenging engineering tasks, but require no technology development. Substantially similar tasks have been repeatedly done for past missions.

Major steps	Cumulative allocation (arc sec HPD)	Cumulative status (arc sec HPD)	Error source	Allocation (arc sec HPD)	Technology status (arc sec HPD)	Notes
Optical prescription	0.11	0.11	Diffraction	0.10	0.10	At 1 keV: weighted mean of diffractions limits of all shells
			Geometric PSF (on-axis)	0.05	0.05	The on-axis design PSF is slightly degraded to achieve best possible off-axis PSF.
Fabrication of mirror segments	0.25	0.55	Mirror Substrate	0.20	0.50	Each pair of mirror segments must produce images better than 0.2 arc sec HPD, based on optical metrology.
			Coating	0.10	0.20	The coating enhancing x-ray reflectance must not degrade the mirror pair PSF by more than 0.1 arc sec
Integration of segments to modules	0.34	1.29	Alignment	0.10	1.10	Each pair's image centroid must be located within 0.1 arc sec of the mirror module's overall image.
			Bonding	0.20	0.40	Bonding of the mirror pair must not degrade the PSF by more than 0.2 arc sec
Integration of modules to metashells	0.36	1.30	Alignment	0.10	0.10	Each module's image is to be located within 0.1 arc sec of the overall metashell image.
			Bonding	0.10	0.10	Bonding must not shift the module's image centroid by more than 0.1 arc sec
Integration of metashells to assembly	0.39	1.31	Alignment	0.10	0.10	Each metashell's image is to be located within 0.1 arc sec of the overall assembly image.
			Attachment	0.10	0.10	Bonding of the metashell must not shift the image centroid by more than 0.1 arc sec
Ground to orbit effects	0.43	1.33	Launch shift	0.10	0.10	Launch disturbance must not degrade the PSF by more than 0.1 arc sec
			Gravity Release	0.10	0.14	Upon reaching orbit when gravity disappears, the mirror assembly's PSF must not degrade by more than 0.1 arc sec
			On-orbit thermal	0.10	0.16	On-orbit thermal disturbance must not degrade the PSF by more than 0.1 arc sec
On-orbit performance (RSS)				0.43	1.33	This is the on-axis performance of the mirror assembly on orbit. Add effects of jitter and detector pixellation to get the final observatory-level PSF.

will determine the thickness of the mirror. What is left to be decided is how to realize the mirror surface area: a small number of very large mirror segments or a large number of small mirror segments or somewhere between the two extremes. See Sec. 3.1 for how we have decided on the mirror segment dimensions for Lynx.

Each mirror segment, together with its primary or secondary counterpart, must meet image and effective area requirements. They also have to meet structural integrity requirement as well so that they will be able to survive the launch.

2.2 Mirror Modules

Each mirror module is composed of dozens of mirror segments precisely aligned and bonded onto a structural element, i.e., a midplate that is made of the same material as the mirror segments. In addition, for reasons of thermal control and minimization of mechanical blockage, we have chosen also to implement stray light baffles on each module. The module construction process must realize the full potential of each mirror segment. In the end, each module must pass x-ray performance tests before and after a battery of environmental tests, including vibrations, thermal vacuum, acoustics, and shock tests.

2.3 Mirror Metashells

Each metashell is composed of a number of identical mirror modules, aligned and bonded onto two integration rings, one at the forward end and the other at the aft end of the module. The forward end of the module's midplate is a precision-ground surface that serves as the reference from which its focal length is defined and measured. The forward ring, as such, serves as a reference for confocality of all modules.

The alignment and bonding of the module into its metashell, while a process demanding engineering precision, requires no special development. This is for two reasons. The first is that the module is a rigid body, consisting of a rigid midplate with dimensions of ~ 200 mm in the optical axis direction by 100 mm in the circumferential direction by 10 mm in thickness or in the radial direction, and many mirror segments, which by some measure enhance the module's structural stiffness. The second reason is that the precision required to align a module is relatively loose, much looser than that required for aligning and bonding a mirror segment in the process of constructing the module. For Lynx the required precision for each of the six degrees of freedom is as follows:

1. Decenter errors (X and Y): These are the location of the module in the $X - Y$ plane that is perpendicular to the optical axis. For a 10-m focal length, the plate scale is $48.5 \mu\text{m}$ per arc sec. To meet the 0.1 arc sec error allocation in Table 2 for this step, the X or Y error needs only to be $0.1 \times 48.5 / \sqrt{2} \approx 3.4 \mu\text{m}$, which can be measured and realized with a high-precision coordinate measuring machine.
2. Despace error (Z): This is the location of the module along the optical axis direction. The focus depth of a module, in the worst case for Lynx, is 3 arc sec per millimeter. To stay below the 0.1 arc sec allocation, the despace error must be smaller than $33 \mu\text{m}$, which is relatively easy to measure and realize.

3. Pitch and yaw errors: These are rotations around axes perpendicular to the optical axis. Since each module is already a two-reflection system, behaving like a thin lens, and that each module has excellent off-axis response, a pitch (or yaw) error of several to tens of arc sec will not materially affect the metashell's angular resolution. These are very loose requirements and can be easily met.
4. Roll error: This is rotation around the center-line of the module parallel to the optical axis. In the worst case for Lynx where the radius of curvature of the module is 1500 mm, the displacement of the module image by a roll angle error is 0.15 arc sec per arc sec. To keep the displacement less than 0.1 arc sec, the roll error must be less than 0.6 arc sec, which is relatively easy to realize for a rigid body such as a module.

Therefore, the integration of a module into its metashell is a straightforward process, though requiring engineering precision and discipline. Substantially similar and even more demanding tasks have been performed for past missions. It should be noted that a significant feature of the module or the metashell is that, other than trace amounts of foreign materials such as mirror coatings and epoxy, they are made of a single material, which in the Lynx case is silicon. This uniformity in material offers significant advantages during their construction process and later during mission operations where the operating temperature of the mirror assembly can differ from the laboratory temperature where they were built and tested.

2.4 Mirror Assembly

The 12 metashells are aligned and attached to a spider-web made of composite material or metal to bear the load of all metashells and to structurally interface to the rest of the observatory. The alignment of a metashell, which is treated as a rigid body, has requirements in X, Y, Z , pitch, yaw similar to those of the module alignment, but it essentially has no roll requirement because of its axial symmetry. The attachment of a metashell to the spider is via a number of titanium flexures, which serve as structural and thermal isolators between the metashells and the rest of the observatory. At the outer edge of the spider-web is a stiff flange that allows the mirror assembly to be mounted to the observatory.

3 Technology Development

Of the several steps required to build the Lynx mirror assembly, only two are unique, have never been done, and therefore require technology development, the others being straightforward engineering exercises. These two steps are the fabrication of mirror segments, and alignment and bonding of mirror segments to make the mirror modules. They are unique to the building of a large x-ray mirror assembly in general and to the building of a mirror assembly for Lynx in particular. They must meet the threefold requirement of angular resolution, light weight, and production cost.

3.1 Mirror Segment Fabrication

We have chosen direct fabrication as the method for making mirror segments because of two considerations. First, of all techniques that have been used for making optics in general and

x-ray optics in particular, direct fabrication, also known as grind-and-polish, makes the best possible optics. Second, direct fabrication technology has progressed by leaps and bounds in the last 20 years since the Chandra mirrors were fabricated in the 1990s. Many then-esoteric techniques have matured and become commercially available in the form of turnkey machines. In particular, ion beam figuring technology has become widely used in the semiconductor industry for making high precision wafers to meet ever more stringent device requirements. Perhaps most important of all, some of these polishing processes exert little to no shear stress or normal pressure that could fracture thin substrates, opening up the possibility of polishing thin optical components that were not possible before.

In conjunction with choosing the direct fabrication method, we have chosen monocrystalline silicon as the material because of several reasons. First of all, monocrystalline silicon is free of internal stress, unlike any other materials, especially glass, that are full of internal stress because of domain boundaries between crystal grains as in metals or because of supercooling as in glass. This lack of internal stress makes it possible to use deterministic material removal techniques of modern polishing technologies to make precision optics: any figure change is determined and only determined by the amount of material removed. In contrast, with a material with internal stress, the removal of material causes figure change in two ways: the disappearance of the material itself and the disappearance or appearance of stress as a result of the material removal. The figure change due to stress is unpredictable. The unpredictable stress-induced figure change is totally negligible for a thick (~ 10 mm) substrate but not so for a thin (~ 0.5 mm) substrate.

Second, silicon has highly preferred material properties. It has a relatively low density, 2.33 g/cm^3 , lower than most glasses and aluminum. Its elastic modulus, $\sim 150 \text{ GPa}$, is twice that of the typical glass and aluminum alloys, making it relatively stiff. Equally important is its high thermal conductivity, 130 W/mK at room temperature, more than 100 times higher than the typical glass, minimizing thermal gradients caused by a hostile thermal environment in space. Compounding the benefit of high thermal conductivity is its low coefficient of thermal expansion, 2.6 ppm/K at room temperature, lower than typical glass and much lower than typical metals. All of these material properties make silicon almost an ideal material for making x-ray mirrors for spaceflight. It would be ideal if its coefficient of thermal expansion were zero.

In addition, monocrystalline silicon is an industrial material. Very large blocks of it are commercially available at low costs. In conjunction with this, material availability is the availability of a large body of knowledge that has been accumulated in the last 50 years and industrial equipment for processing it. No other material enjoys these advantages. As a matter of fact, a key aspect of our technology development is to maximize the use of these advantages to make the best x-ray optics at the lowest possible cost.

Once the fabrication technique and material are determined, the thickness of the mirror segment can be determined by three parameters: mass allocated for the mirror assembly, mirror surface area, and density of the material. For Lynx, these three parameters lead to a thickness of 0.5 mm . The dimensions of the mirror segment are then determined by finite element analysis requiring that gravity distortion while the mirror is supported at four locations (see Sec. 3.2) and is sufficiently small to meet angular resolution requirements. All things considered,

the dimensions of the mirror segment are determined to be $100 \text{ mm} \times 100 \text{ mm} \times 0.5 \text{ mm}$. This size happens to be similar to a 150 mm in diameter wafer that is commonly produced and processed by the semiconductor industry, enabling us to use commercially available equipment and silicon blocks to facilitate mirror segment production and to minimize cost.

3.1.1 Mirror substrate fabrication

The mirror substrate fabrication process,^{19–23} shown in Fig. 2, starts with a commercially procured block of monocrystalline silicon, measuring $150 \text{ mm} \times 150 \text{ mm} \times 75 \text{ mm}$, shown in the upper-left panel. In the next step, upper-middle panel of Fig. 2, a conical approximation contour is cut with a band saw into the block, which is then lapped on a precision conical tool to generate a precision conical surface that is a zeroth- and first-order approximation to an x-ray mirror segment. Then, the block is brought back to the band saw again to slice off a thin silicon shell, as illustrated in upper-right panel of Fig. 2. This silicon shell, because of the cutting and lapping process, has damage to its crystal structure. To remove the damage, it is etched in a standard industrial process with an HNA solution, a mix of hydrofluoric acid, nitric acid, and acetic acid. After this etching step, the thin shell is a single crystal where practically every atom is on its lattice location. The entire shell is free of any internal stress. At this point, the shell's surface is rough and not capable of reflecting x-rays at all, let alone forming images.

Then, the conical substrate is polished with synthetic silk on a cylindrical tool to achieve required specularly and micro-roughness. In order for the reciprocity to be random in both the circumferential direction and axial direction to avoid grooving, the conical substrate is elastically bent into a cylindrical shape during polishing. This is equivalent to stress-polishing that was successfully used for making aspheric mirrors for the Keck telescopes. This step results in a mirror substrate whose clear aperture is $\sim 100 \text{ mm} \times 100 \text{ mm}$, with roll-off errors near the four edges that are typical of full-aperture polishing processes, shown in the lower-middle panel of Fig. 2. The areas near the edges are removed on a dicing saw, resulting in a mirror substrate of the required size, shown in the lower-right panel of Fig. 2. The monocrystalline nature of the substrate is such that the figure of the remaining mirror does not change at all as a result of the operation.

The final step of the mirror substrate fabrication is a figuring process using an ion beam. The mirror substrate is measured on an interferometer to produce a topographical map that is used to guide the ion beam to preferentially remove material where the surface is high. As of October 2018 many mirror substrates have been fabricated. Figure 3 shows the parameters of one of the best mirror substrates produced. Its overall quality is similar to Chandra's mirror. Two mirrors like this one, when properly aligned, are predicted to achieve images of 0.5 in. HPD at 1 keV . In the coming years, every step of the entire substrate fabrication process will be examined, refined, and perfected to achieve better substrates, reaching the diffraction limit by sometime in the middle of the 2020s. We expect to be able to make substrates meeting Lynx requirements by the end of 2019.

3.1.2 Mirror coating

Bare silicon surface is a poor x-ray reflector. It needs to be coated with thin films to enhance its reflectivity. There are potentially many different ways of coating the bare silicon

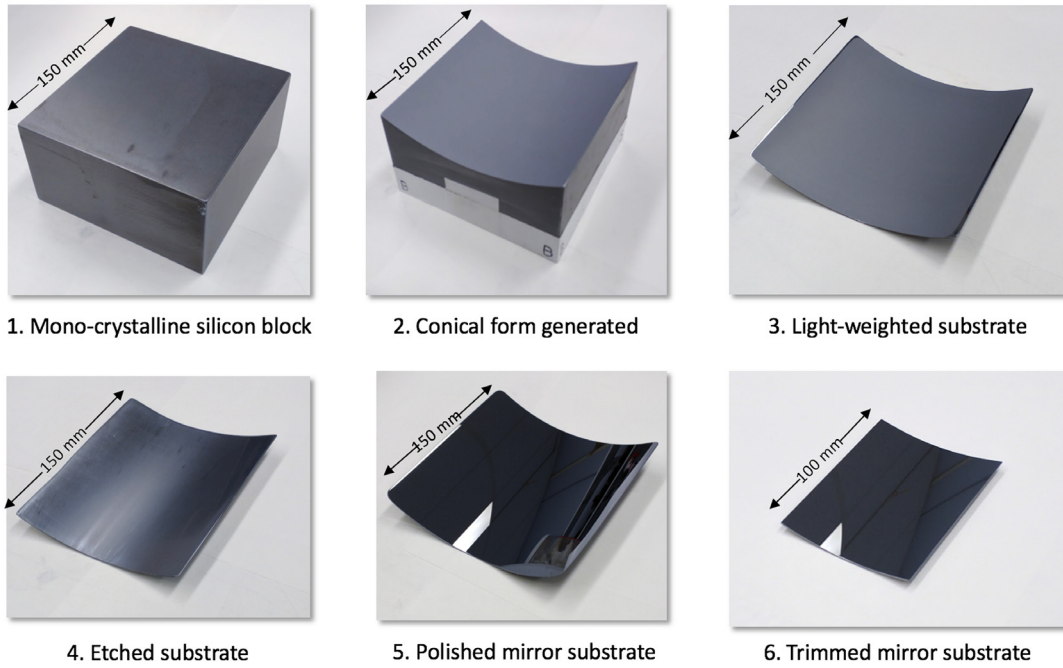


Fig. 2 Six major steps of fabricating a mirror substrate. This entire process, using no special equipment other than what is commonly available, takes about 15 h labor time and 1 week of calendar time. The process is highly amenable to automation and mass production methods, leading to high throughput and low cost.

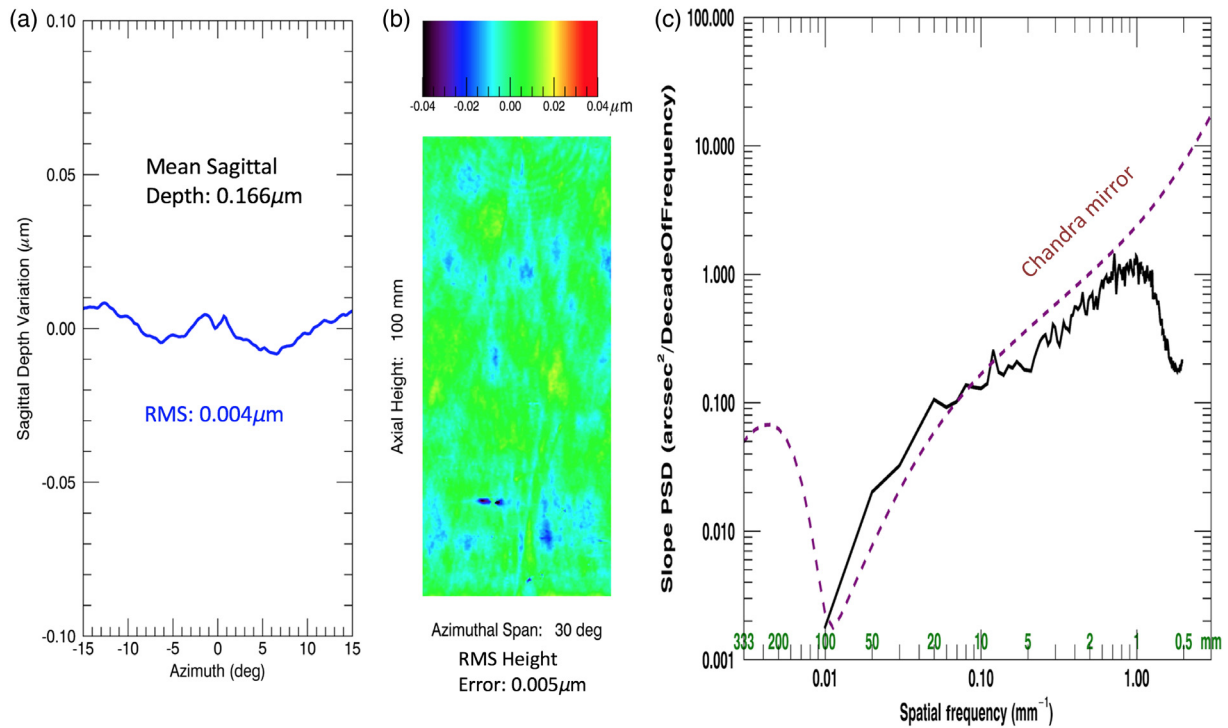


Fig. 3 Measured properties of a finished mirror substrate. (a) sagittal depth variation as a function of azimuth. This substrate's average sagittal depth of 166 nm differs from the design value of 174 nm by 8 nm. The RMS variation of the sagittal depth is 4 nm. (b) Surface error topography. After removal of the sagittal depth, this mirror has an RMS height error of only 5 nm. (c) Slope power spectral density (black solid curve) in comparison with Chandra's mirror (dashed curve). All of the errors combine to make this mirror substrate have an image quality of 0.5 arc sec HPD (two reflection equivalent).

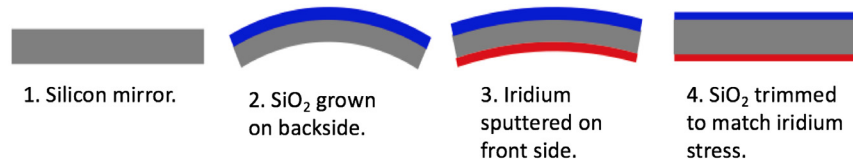


Fig. 4 Illustration of mirror coating process to enhance x-ray reflectance while preserving the figure quality of silicon substrate. The distortion caused by the stress of the iridium thin film is precisely balanced or compensated for by the stress of the silicon oxide on the other side of the mirror substrate.

surface to achieve high reflectance, but for the purpose of this technology development, we assume the use of the traditional iridium coating. Other coatings, when fully demonstrated, can be implemented with little to no change to the process presented here. The major issue related to coating is the fact that coating introduces stress that can severely distort the figure of a mirror substrate.²⁴ The preservation of the substrate figure requires a way to cancel or otherwise compensate for its effect.

The coating process, shown in Fig. 4, starts with a bare silicon substrate cleaned of particulate and molecular contaminants. Using the standard semiconductor industry's dry oxide growth process, we coat the backside, i.e., the convex side or the nonreflecting side, with a layer of SiO₂. The SiO₂ exerts compressive stress on the substrate, causing it to distort as shown in Fig. 4 (step 2). Then, a thin film of iridium, with an undercoat of chrome serving as a binding layer, is sputtered on the front side. The compressive stress of the iridium film counteracts the SiO₂ stress, canceling some of the distortion, shown in Fig. 4 (step 3), but still, significant distortion remains. The final step is to trim the thickness of the SiO₂ layer thickness to achieve precise cancellation of stresses and restore the figure of the substrate. The trimming is guided by precise figure measurement and finite element analysis.

One way of trimming the thickness of the SiO₂ layer is using chemical etching. This has been recently demonstrated.²⁵ Another way of trimming is using an ion beam, the same as figuring the silicon substrate. Since this is a dry process, as opposed to the wet chemical etching process, it has the advantage of being cleaner. We expect this to be experimented with in 2019.

3.2 Mirror Alignment

A mirror segment needs to be aligned and bonded to form part of a mirror module. We have chosen to support a mirror segment at four optimized locations,²⁶ as shown in Fig. 5. Four supports, as in the case of three supports for a flat mirror, necessarily and sufficiently determine the location and orientation of a curved mirror, such as an x-ray mirror. Using gravity, or the weight of the mirror segment, as the nesting force, the alignment of the mirror segment is determined by the heights of the four supports,

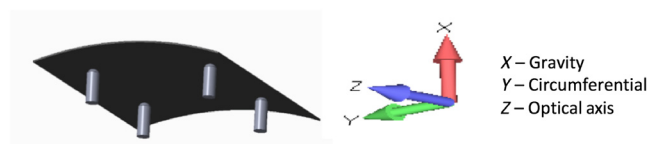


Fig. 5 Illustration of the four-point kinematic support of an x-ray mirror. The four supports are approximately located one quarter way inboard from each corner. See text for a discussion of the advantages of aligning and bonding a mirror segment using these four supports, which are also called spacers or posts.

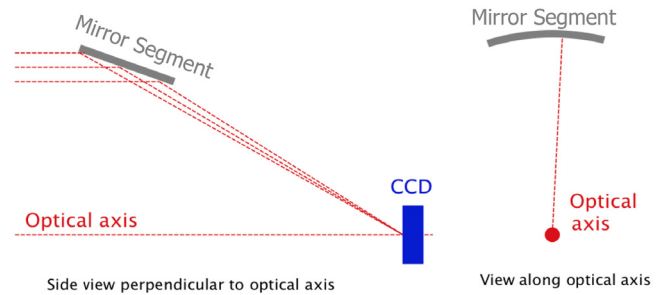


Fig. 6 Illustration of the Hartmann setup using a beam of visible light to measure the location and orientation of the mirror segment being aligned.

which are interchangeably called posts or spacers. The alignment task is reduced to the precision grinding of the heights of these spacers.

The alignment process is an iteration of Hartmann measurement²⁷ using a beam of visible light monitored by a CCD camera, shown in Fig. 6, and precision grinding of the heights of the spacers. The precision of the spacer heights required depends on the radius of curvature of the mirror segment. In the worst case for Lynx for the largest radius of curvature of 1500 mm, the 0.1 arc sec alignment error budgeted in Table 2 translates into a spacer height error of 25 nm. With a deterministic grinding or material removal process, this precision is easily achievable. In the course of the last 2 years, we have repeatedly aligned many mirror segments, both primary and secondary ones individually, and primary and secondary segments combined. We have been able to achieve alignment accuracy of ~ 1 arc sec. HPD, which is dominated by the diffraction effect of the visible light, limiting the precision of alignment determination. Our plan is to refine this process by using visible light of a shorter wavelength to minimize the diffraction effect to achieve 0.1 arc sec alignment precision.

3.3 Mirror Bonding

Bonding the mirror segment is a direct and easy extension of the alignment process. Once the four spacers have the correct heights as determined by the Hartmann measurement, the mirror segment is removed, a small amount of epoxy is applied to the top of each of the four spacers, and then the mirror segment is placed on them again. Finally, vibrations are applied to help the mirror segment settle in its optimal configuration, the same way as during the iterative alignment process. During the settling process, because of the weight of the mirror and the vibrations, the epoxy on each spacer is spread and compressed. The mirror segment is permanently bonded when the epoxy completes curing.²⁵

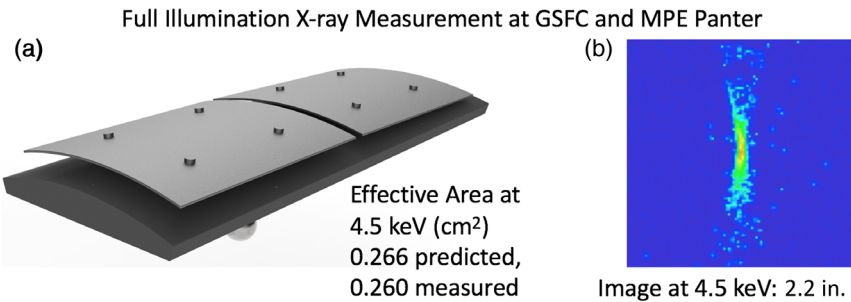


Fig. 7 (a) A pair of mirrors aligned and bonded on a silicon plate. Each mirror is bonded at four locations with silicon spacers (not visible in this view). The four spacers on the back of each of the two mirrors are therefore the next pair of mirrors. (b) An x-ray image obtained with a beam of 4.5 keV (Ti K) x-rays, with a half-power diameter of 2.2 in.. The effective areas at several energies are measured at MPE's Panter x-ray beam line, thanks to Dr. Vadim Burwitz and his team, to agree with theoretical expectations.

This way of supporting and bonding the mirror segment has many advantages. First, the gravity-induced distortion is not frozen in permanently. Because of the optimization of the locations of the four spacers, the gravity distortion disappears once the gravity is released. Second, the epoxy bonds do not affect the alignment of the mirror segment. Third, any local distortion caused by epoxy cure is minimal as the diameter of the spacer is only a few times larger than the thickness of the mirror segment. The mirror segment, being 0.5 mm in thickness, is very stiff over the length scale of several millimeters similar to the diameter of the spacers.

The validity of the entire process, from mirror substrate fabrication to alignment and bonding, has been demonstrated by successfully building and testing mirror modules repeatedly as shown in Fig. 7. It was placed in the 600-m x-ray beam line at the Goddard Space Flight Center and produced images with 2.2 in. HPD, as shown in Fig. 7(b). The same module was also tested at the Panter 100-m x-ray beam line and measured for its effective areas at several different energies, agreeing within 2% with calculations based on atomic form factors independently measured.

3.4 Building and Testing Mirror Modules

Building a mirror module is just many repetitions of the process described in Secs. 3.1, 3.2, and 3.3: fabrication, coating, aligning, and bonding of one mirror after another, as shown in Fig. 8. In the middle of the stack of mirror pairs is a thick silicon plate, annotated as flight plate, in Fig. 8, that will be a permanent part of the module and will be used as the load-bearing structure to align and bond the module to the metashell. The interim plate in Fig. 8, on the other hand, is a piece of ground support equipment and will be removed once the module construction is complete. It should be noted that this way of aligning and bonding one mirror segment is free of any stack-up errors as each mirror segment is aligned without referencing to any other mirror segment that has already been bonded. The mirror segments previously bonded underneath the current one only serve as a structural support. This prevention of any stack-up errors allows each mirror segment to realize its own full potential. It also allows a pair of mirrors to be optimized. Another feature of every module is that, as part of its construction process, it carries a reference from which to measure its focal length, as shown in Fig. 8, step 1.

Each module is individually tested in an x-ray beam for science performance, such as angular resolution and effective area,

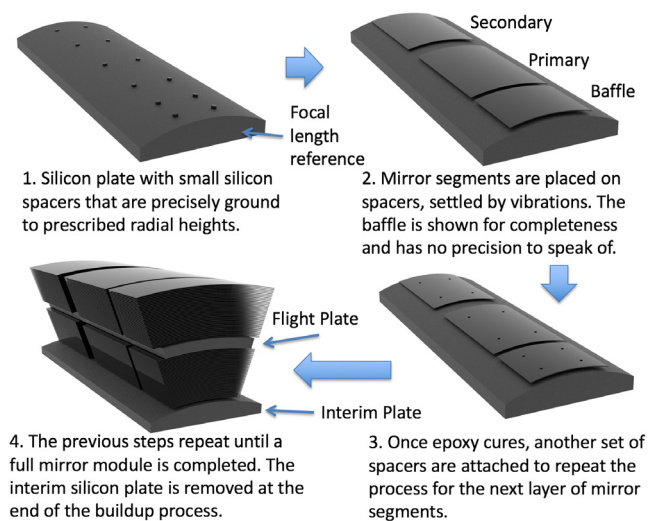


Fig. 8 Building-up of a mirror module. It is a repetition of fabrication, alignment, and bonding of one mirror segment after another. The interim plate is for the construction process only. It will be removed before the module is integrated into a metashell with the flight plate as its load-bearing structure and focal length reference.

both before and after a battery of environmental tests, including vibration, thermal-vacuum, acoustic, and shock tests. One significant advantage of our hierarchical approach is that each module is small in size and weight and therefore can be handled and tested easily, without the need for any special and expensive equipment or test facility. In particular, since each module has many identical copies, managing spares is easily done by making one or two additional modules of each prescription.

3.5 Progression Toward Fully Meeting Lynx Requirements

The process of building and testing mirror modules described in the Sec. 2 will be continually refined and perfected in the next few years to meet all requirements: science performance, space-flight environments, production schedule, and production cost. Table 2 shows the three-pronged strategy to mature this technology. The three prongs are building and testing modules of progressively more mirror segments and meeting progressively more stringent requirements. Many process parameters will be investigated and optimized. Among them are:

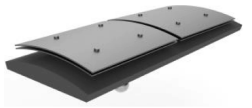
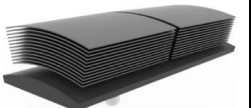
	TRL-4	TRL-5	TRL-6
Illustration			
Description	Fabrication, alignment, and bonding of single pairs of mirror segments to achieve progressively better PSF, culminating in 0.3" HPD.	Alignment and bonding of two or three pairs of mirror segments to achieve progressively better PSF, culminating in 0.3" HPD. Demonstration of the structural and other environmental integrity of the mirror bonds.	Alignment and bonding of many (>3) pairs of mirror segments to achieve progressively better PSF, culminating in 0.3" HPD, passing all environmental tests. Meeting preliminary production throughput and cost requirements.
Objectives	1. Develop and verify mirror fabrication and mirror coating processes. 2. Develop and verify the basic elements of alignment & bonding procedures for precision and accuracy.	1. Develop and verify mechanics and speed of co-alignment and bonding processes. 2. Conduct environmental tests: vibration, thermal vacuum, and acoustic to verify structural and performance robustness.	1. Develop and verify all aspects of module production process: mirror fabrication, coating, alignment, and bonding. 2. Validate production schedule and cost estimates. 3. Develop and plan for mass production.
Status as of 2018	Repeated building and testing, achieving ~2" HPD.	Built and tested one module, achieving ~3" HPD.	In progress.
Expected Date to Meet Lynx Requirements	December 2020	December 2022	December 2024

Fig. 9 A summary of the mirror technology status and plan to meet Lynx requirements. Our objective is to develop and perfect a process that can repeatedly and reliably build and test mirror modules that at least meet and possibly exceed Lynx requirements in the coming years: angular resolution as good as 0.3 arc sec. HPD, effective areas agreeing with expectations, mass, and production throughput and cost.

1. Amount of time that each mirror substrate is polished to achieve optimal figure quality and microroughness,
2. Number of iterations on an ion beam figuring machine to achieve the best possible figure and microroughness,
3. Different coatings, their stress characteristics, and reflectance,
4. Epoxy cure time and strength,
5. Effect of the spacer diameter on bond strength and residual local distortion of the mirror segment, and
6. Optimal number of mirror segments of a module.

4 Summary

We have described an approach to building an x-ray mirror assembly for the Lynx mission. Recent work and x-ray tests have demonstrated the basic validity of this approach. Much remains to be done, however, to optimize and refine the many steps to achieve the best possible science performance, i.e., angular resolution and effective area, with the highest efficiency and lowest possible costs. In addition, many engineering issues need to be adequately addressed to retire or minimize both technical and programmatic risks. Among these issues is the optical prescription for Lynx.

At the outset, it should be noted that the approach we have described is capable of implementing every possible optical

prescription. In other words, which optical prescription to use for Lynx is not a technology problem. Rather it is an optimization problem that needs to be addressed in the broader context of on- and off-axis angular resolution, on- and off-axis effective areas, and stray-light baffling, and other science performance desirements. By default, we have adopted an optical prescription based on the Wolter–Schwarzschild²⁸ design, with modification²⁹ to achieve better off-axis angular resolution. It is possible that other prescriptions, such as the hyperboloid-hyperboloid³⁰ design, or the equal-curvature³¹ design, or the polynomial design,³² can be slightly preferred under some considerations. For the approach we have described, a decision for the final optical prescription can be made shortly before the start of production, which is another advantage of this approach.

We believe that this approach not only holds the promise of meeting Lynx requirements but also holds the promise of achieving much better angular resolution than the subarcsecond angular resolution required by Lynx. It is possible, even likely, that this approach can make diffraction-limited x-ray optics for astronomy before the end of the 2020s (Fig. 9).

Acknowledgments

This work has been funded in part by NASA through the Goddard Space Flight Center's Internal Research and Development funds, the Astronomy and Physics Research and Analysis (APRA) program, and the Strategic Astrophysical Technology (SAT) program.

References

1. R. Giacconi and B. Rossi, "A telescope for soft x-ray astronomy," *J. Geophys. Res.* **65**, 773–775 (1960).
2. L. P. Van Speybroeck, "Design, fabrication and expected performance of the HEAO-B x-ray telescope," *Proc. SPIE* **0106**, 136–143 (1977).
3. B. Aschenbach, "Design, construction, and performance of the ROSAT high-resolution x-ray mirror assembly," *Appl. Opt.* **27**, 1404–1413 (1988).
4. G. Matthews et al., "Mirror cell design, fabrication, assembly, and test for the AXAF VETA-I optics," *Proc. SPIE* **1742**, 191–202 (1992).
5. L. P. Van Speybroeck, "Performance expectation versus reality," *Proc. SPIE* **3113**, 89 (1997).
6. P. A. J. De Kort et al., "The x-ray imaging telescopes on EXOSAT," *Space Sci. Rev.* **30**, 495–511 (1981).
7. P. J. Serlemitsos et al., "The x-ray telescope onboard Suzaku," *Publ. Astron. Soc. Jpn.* **59**, S9–S21 (2007).
8. O. Citterio et al., "Optics for the x-ray imaging concentrators aboard the x-ray astronomy satellite SAX," *Appl. Opt.* **27**, 1470–1475 (1988).
9. P. Gondoin et al., "X-ray spectroscopy mission (XMM) telescope development," *Proc. SPIE* **2209**, 438–450 (1994).
10. B. Aschenbach et al., "Imaging performance of the XMM-Newton x-ray telescope," *Proc. SPIE* **4012**, 731–739 (2000).
11. D. N. Burrows et al., "Swift x-ray telescope," *Proc. SPIE* **4140**, 64–75 (2000).
12. J. Eder et al., "How eROSITA was made," *Proc. SPIE* **10699**, 106991Z (2018).
13. M. Gubarev et al., "The Marshall space flight center development of mirror modules for the ART-XC instrument aboard the spectrum-Roentgen-gamma mission," *Proc. SPIE* **8443**, 84431U (2012).
14. W. W. Zhang, "Manufacture of mirror glass substrates for the NuSTAR mission," *Proc. SPIE* **7437**, 74370N (2009).
15. W. W. Craig, "Fabrication of the NuSTAR flight optics," *Proc. SPIE* **8147**, 81470H (2011).
16. R. Mushotzky, "AXIS: a probe class next generation high angular resolution x-ray imaging satellite," *Proc. SPIE* **10699**, 1069929 (2018).
17. W. W. Zhang et al., "Next generation x-ray optics: high-resolution, light-weight, and low-cost," A paper submitted to NASA in response to solicitation NNH11ZDA018L (2011).
18. J. A. Gaskin et al., "The Lynx x-ray observatory: concept study overview and status," *Proc. SPIE* **10699**, 106990N (2018).
19. R. E. Riveros et al., "Fabrication of single crystal silicon mirror substrates for x-ray astronomical missions," *Proc. SPIE* **9144**, 914445 (2014).
20. R. E. Riveros et al., "Fabrication of high resolution and lightweight monocrystalline silicon x-ray mirrors," *Proc. SPIE* **9603**, 96030W (2015).
21. R. E. Riveros et al., "Progress on the fabrication of high resolution and lightweight monocrystalline silicon x-ray mirrors," *Proc. SPIE* **9905**, 990521 (2016).
22. R. E. Riveros et al., "Progress on the fabrication of lightweight single-crystal silicon x-ray mirrors," *Proc. SPIE* **10399**, 103990T (2017).
23. R. E. Riveros et al., "Fabrication of lightweight silicon x-ray mirrors for high-resolution x-ray optics," *Proc. SPIE* **10699**, 106990P (2018).
24. W. W. Zhang et al., "Constellation-x mirror technology development," *Proc. SPIE* **7011**, 701103 (2008).
25. Y. Yao et al., "Thermal oxide patterning method for compensating coating stress in silicon x-ray telescope mirrors," *Proc. SPIE* **10699**, 1069942 (2018).
26. K. W. Chan et al., "Alignment and bonding of silicon mirrors for high resolution astronomical x-ray optics," *Proc. SPIE* **10699**, 1069940 (2018).
27. T. Saha et al., "Grazing incidence wavefront sensing and verification of x-ray optics performance," *Proc. SPIE* **8147**, 814717 (2011).
28. H. Wolter, "Generalized Schwarzschild systems of mirrors with glancing reflection as optical systems for x-rays," *Ann. Phys.* **10**, 286–295 (1952).
29. T. T. Saha, "Optical design for a survey x-ray telescope," *Proc. SPIE* **9144**, 914418 (2014).
30. J. E. Harvey et al., "Hyperboloid-hyperboloid grazing incidence x-ray telescope designs for wide-field imaging applications," *Proc. SPIE* **4012**, 328 (2000).
31. T. T. Saha and W. W. Zhang, "Equal-curvature grazing-incidence x-ray telescopes," *Appl. Opt.* **42**, 4599–4605 (2003).
32. C. J. Burrows et al., "Optimal grazing incidence optics and its application to wide-field x-ray imaging," *Astrophys. J.* **392**, 760–765 (1992).

Biographies of authors are not available.